PHYSICAL REVIEW C **66**, 044006 (2002)

Pseudovector vs pseudoscalar coupling in one-boson exchange *NN* potentials

G. Caia,[1] J. W. Durso,[2] Ch. Elster,[1,2] J. Haidenbauer,[2] A. Sibirtsev,[2] and J. Speth[2]
[1]*Department of Physics and Astronomy, Ohio University, Athens, Ohio 54701*
[2]*Institut für Kernphysik (Theorie), Forschungszentrum Jülich, D-52425 Jülich, Germany*
(Received 3 May 2002; published 25 October 2002)

We examine the effects of pseudoscalar and pseudovector coupling of the π and η mesons in one-boson exchange models of the *NN* interaction using two approaches: time-ordered perturbation theory unitarized with the relativistic Lippmann-Schwinger equation, and a reduced Bethe-Salpeter approach using the Thompson equation. Contact terms in the one-boson exchange amplitudes in time-ordered perturbation theory lead naturally to the introduction of *s*-channel nucleonic cutoffs for the interaction, which strongly suppresses the far off-shell behavior of the amplitudes in both approaches. Differences between the resulting *NN* predictions of the various models are found to be small, and particularly so when coupling constants of the other mesons are readjusted within reasonable limits.

DOI: 10.1103/PhysRevC.66.044006 PACS number(s): 13.75.Cs, 21.30.Cb, 21.30.Fe

I. INTRODUCTION

Since the discovery and identification of the pion [1,2] as the strongly interacting meson anticipated by Yukawa [3] in 1935, most theoretical efforts to construct a quantitatively accurate model of the nucleon-nucleon (*NN*) interaction have used the pion-nucleon interaction as the first building block. Indeed, phase shift analyses of *NN* scattering data since 1959 [4] use the one-pion exchange amplitude to fix the phase shifts of the high orbital angular momentum partial waves, which are not individually adjusted to fit the data.

Almost at the beginning of these efforts the question arose of whether the fundamental coupling of the pion to the nucleon is of the pseudovector or pseudoscalar type. The question arises, of course, from the fact that the fully on-shell one-pion exchange amplitude derived from a πNN interaction Lagrangian with pseudovector coupling is identical in form to that from one with pseudoscalar coupling. In early attempts to go beyond the one-pion exchange to the two-pion exchange [5,6], pseudoscalar coupling appeared to demand suppression of ''pair terms''—terms describing the contribution from intermediate states with one or more antinucleons. For the exchange of pions with low momenta, this effectively reduced to pseudovector coupling, for which the renormalizability of the theory is doubtful, at best [7,8]. Pion-nucleon scattering, through the smallness of the scattering lengths, also strongly suggested pseudovector coupling. Dispersion-theoretic results for the two-pion exchange contribution [9,10] based on unitarity and analytic continuation of πN amplitudes to the $\pi\pi \rightleftharpoons N\bar{N}$ channel also implicitly favored pseudovector coupling.

We realize now that the meson theory of nuclear forces is not a fundamental theory but, at best, an effective theory. Thus lack of renormalizability in the usual sense is not a relevant criterion for the rejection of one form of coupling or another. Furthermore, the approximate chiral symmetry exhibited by QCD and implemented with considerable success in chiral perturbation theory (χPT) [11] makes it clear that the effective coupling of pions to nucleons, at least at low energies, is pseudovector in character. In other phenomena the picture is more complex. In pion electro- and photoproduction analyses at low energies pseudovector coupling is preferred, whereas at higher energies pseudoscalar coupling provides a more economical description [12,13]. In the light of this evidence it is clear that any of the *NN* interaction models claiming to be realistic should, to some degree, include pion exchange with pseudovector coupling.

With the exception of some recent models based on baryon χPT [14–18], *NN* models of the past three decades include, in addition to the one-pion exchange, contributions due to exchange of heavier mesons, whether explicitly, as in the various one-boson exchange (OBE) models [19–28], or implicitly, as resonant *t*-channel exchange of two pions, as in the dispersion-theoretic approaches [9,10]. Even within the OBE models there is no single preferred approach. There are those models that are based on a Bethe-Salpeter [29] approach and in which the unitarizing equation is some three-dimensional reduction of the Bethe-Salpeter equation [22,30–32,25–27], and there are those, including some of the various Bonn potentials [25,28,33], that are based on time-ordered perturbation theory (TOPT). Our main interest in this work is in TOPT, but we shall also examine differences between pseudoscalar and pseudovector coupling in both of these approaches. For that purpose we will utilize a specific three-dimensional reduction of the Bethe-Salpeter equation known as the Thompson equation [31].

In covariant perturbation theory one starts with a Lorentz-invariant Lagrangian density, from which one derives the Hamiltonian density and, from that, the Hamiltonian. For Lagrangians with scalar or pseudoscalar mesons without derivative coupling, the interaction part of the Hamiltonian density is just the negative of the interaction part of the Lagrangian density. For Lagrangians with derivative coupling or with vector mesons, however, noncovariant ''contact'' terms arise in the Hamiltonian density. These terms are necessary to cancel the noncovariant terms in the meson propagators so that, in any order of perturbation theory, the resulting amplitude is covariant [34]. From a procedural point of view, this means that in the Feynman rules one simply drops the contact terms and the noncovariant parts of the propagators.

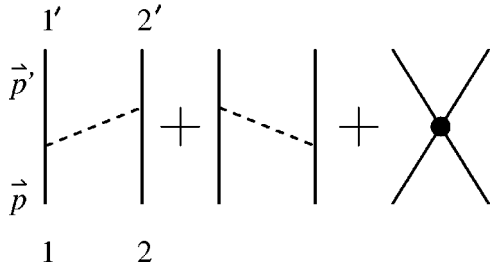

FIG. 1. Schematically, the three terms in time-ordered perturbation theory that may contribute to *NN* scattering in second order of the coupling constant in a meson exchange model.

In TOPT, however, one does not use particle propagators. They are effectively supplied by the vertex functions and energy denominators in the time-ordered diagrams. In order to obtain covariant results in TOPT starting from a Lagrangian density with derivative coupling, or with vector mesons, one must include the contributions of the contact interactions in the Hamiltonian in the appropriate order of the perturbation expansion. Therefore, for single pion exchange with pseudovector coupling in *NN* scattering, i.e., in second order in the coupling constant, one must include not just the meson exchange diagrams, but also the four-point *NN* contact interaction, as shown in Fig. 1, and similarly for vector meson exchange. Only then will the result agree with covariant perturbation theory when all external particles are on their mass shells.

The main focus of the work that follows is to compare the results of inclusion of the full pseudovector-coupled pion exchange with those of pseudoscalar coupling in one-boson exchange models based on time-ordered perturbation theory. This is not simply a moot point: the pion-nucleon interaction used in Ref. [33], although nominally of pseudovector type, is in fact pseudoscalar, and thus has a very different off-energy shell behavior from pseudovector coupling. Furthermore, contact terms in the vector meson exchange contributions, as well as gauge terms, which have heretofore been ignored, will be retained.

We shall, in this work, restrict ourselves to examining one-boson exchange models, since the contact terms in higher orders of TOPT present additional difficulties that are not easily resolved. We will, as in all models of this kind, need to introduce cutoffs in order to ensure convergence of the integral equations used to unitarize the scattering amplitude. We will also compare the results to those obtained from a reduced Bethe-Salpeter approach, in which the problem of contact terms does not arise.

In Sec. II we describe the models that we employ in the present study. In particular, we give the equations that are used for unitarizing the scattering amplitude and we discuss some specific aspects of the vertex form factors. Finally, we outline the strategy that was followed for fixing the free parameters of the models. Results for phase shifts as well as for the deuteron properties are presented in Sec. III. We analyze the consequences of pseudovector versus pseudoscalar coupling in TOPT as well as in a model based on the Thompson equation and we also compare the different approaches. In Sec. IV we summarize our results and draw some conclusions. Technical details such as the underlying Lagrangians, and the potential matrix elements in TOPT and for the Thompson equation, are summarized in Appendixes A, B, and C.

TABLE I. Quantum numbers and masses of the mesons used in the models in this work.

Meson	$I(J^P)$	Mass (GeV)
π	$1\ (0^-)$	0.138 03
η	$0\ (0^-)$	0.5488
σ	$0\ (0^+)$	0.52
a_0	$1\ (0^+)$	0.983
ρ	$1\ (1^-)$	0.769
ω	$0\ (1^-)$	0.7826

II. MODELS

In order to make the comparison of different treatments of pseudoscalar meson exchange explicit we will focus on four one-boson exchange models of the *NN* interaction. The first model that we will consider is that of pseudovector coupling of the pseudoscalar mesons, π and η, in TOPT. The second will be the same with the exception that pseudoscalar coupling of the pseudoscalar mesons will be used. For the third and fourth models we make the same comparison of pseudovector and pseudoscalar coupling for the pseudoscalar mesons, but within a Bethe-Salpeter approach to the problem using the Thompson equation [31] to unitarize the scattering amplitude.

The roster of exchanged mesons in each of the four models is identical: pseudoscalar mesons π and η, vector mesons ρ and ω, and scalar mesons σ and a_0. Contact terms as well as gauge terms arising in the polarization sums in vector meson exchange in TOPT will be retained. In the reduced Bethe-Salpeter approach, gauge terms in the vector meson propagators will also be retained. The masses and quantum numbers of the mesons are given in Table I.

The interaction Lagrangian densities for all of the meson-baryon interactions in our model calculations are given in Appendix A, along with the corresponding Hamiltonian densities. The matrix elements of the corresponding second order potentials for the TOPT-based models are presented in Appendix B. Shown schematically in Fig. 2 are the interaction and the kinematics for the potential V in the *NN* center-of-mass frame. For this we unitarize the scattering amplitude through use of the Lippmann-Schwinger equation,

$$\mathbf{T}=\mathbf{V}+\mathbf{V}\frac{1}{W-\mathbf{H}_0+i\epsilon}\mathbf{T} \tag{1}$$

or, more precisely,

$$\begin{aligned}\langle \vec{p}\,'\lambda_1'\lambda_2'|T(W)|\vec{p}\lambda_1\lambda_2\rangle &= \langle \vec{p}\,'\lambda_1'\lambda_2'|V(W)|\vec{p},\lambda_1\lambda_2\rangle + \sum_{\mu_1\mu_2}\int \frac{d^3q}{W-2E_q+i\epsilon} \\ &\times \langle \vec{p}\,'\lambda_1'\lambda_2'|V(W)|\vec{q}\mu_1\mu_2\rangle\cdot\langle \vec{q}\mu_1\mu_2|T(W)|\vec{p}\lambda_1\lambda_2\rangle.\end{aligned} \tag{2}$$

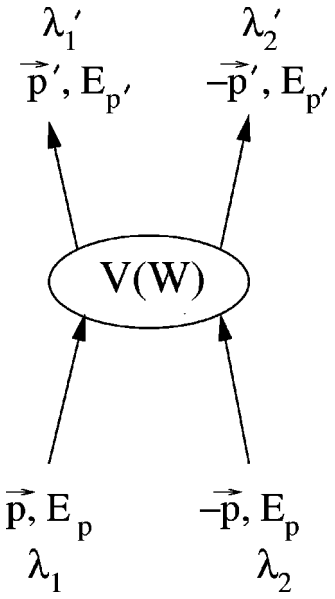

FIG. 2. Kinematics for the *NN* potential in the *NN* center-of-mass frame with total energy **W**. The fermion lines are labeled by their three-momentum, energy, and helicity.

Here W represents the total energy of the NN system.

The Thompson equation, which we use to unitarize the scattering amplitude in the other two models, is given by

$$\langle \vec{p}\,'\lambda_1'\lambda_2'|\mathcal{T}(W)|\vec{p}\lambda_1\lambda_2\rangle = \langle \vec{p}\,'\lambda_1'\lambda_2'|\mathcal{V}(W)|\vec{p},\lambda_1\lambda_2\rangle + \sum_{\mu_1\mu_2}\int \frac{d^3q}{W-2E_q+i\epsilon} \times \langle \vec{p}\,'\lambda_1'\lambda_2'|\mathcal{V}(W)|\vec{q}\mu_1\mu_2\rangle \cdot \frac{m_N^2}{E_q^2}\langle \vec{q}\mu_1\mu_2|\mathcal{T}(W)|\vec{p}\lambda_1\lambda_2\rangle. \tag{3}$$

The simple prescription for obtaining the matrix elements $\mathcal{V}$ from the matrix elements $V(W)$ of Eq. (2) is given in Appendix C. The relations between the standard NN phase parameters and the matrix elements of T can be found in Appendix C.2 of Ref. [33]. We wish to point out here that this relation applies to both of the models employed, taking into account the transformation $T=(m_N/E_{p'})\cdot\mathcal{T}\cdot(m_N/E_p)$ for the models based on the Thompson equation.

Except for the cutoff functions $F_j(W,\vec{p}\,',\vec{p})$ that multiply the field-theoretic meson exchange amplitudes in the potential matrix elements V and $\mathcal{V}$, the input to our model calculations is completely specified. The cutoff functions, as already mentioned, are needed for the convergence of the scattering equation, but the form that one chooses is largely arbitrary. One commonly used, especially in one-boson exchange models, is the so-called ''multipole'' form,

$$F_j(W,\vec{p}\,',\vec{p}) = \left[\frac{\Lambda_j^2-m_j^2}{\Lambda_j^2+(\vec{p}\,'-\vec{p})^2}\right]^{n_j}, \tag{4}$$

where Λ_j and n_j are the free parameters and m_j stands for the meson mass. Part of the appeal of this particular cutoff is that the connection between the range at which the cutoff becomes effective for that meson potential is simply related to the cutoff parameter: $R_{j,\mathrm{cutoff}}\approx\sqrt{n_j}/\Lambda_j$. Considered as a product of two mesonic form factors, this is then interpreted as, or assumed to be, a reflection of the effective size of the meson cloud in that part of the NN interaction.

In treating contact terms in the interaction, however, this form immediately raises some difficulties. The first is that, through the dependence on the three-momentum transfer in the denominator, it introduces effects of the contact terms into *all* angular momentum partial waves, whereas the contact terms alone, which are polynomials of low degree in the sine or cosine of the c.m. scattering angle, contribute only to a few of the lowest partial wave amplitudes. The contact term arising from pseudovector pion coupling, for example, contributes only to *s* and *p* waves. In adopting the multipole form, one singles out the three-momentum transfer as the variable in which to cut off the potential, but there is no compelling reason to do so, and good reason not to. Indeed, in the effective field theoretic approach of Epelbaum *et al.* [15], a purely *s*-channel cutoff is used.

On the other hand, we wish to have the comparison presented in this work make some contact with models in the literature [24,25,33] that employ *t*-channel cutoffs. Furthermore, we wish to apply the same cutoff to both the meson exchange terms *and* the contact terms in order that one term not receive excessive weight from one kinematic region in the range of the loop integral as compared with the other. This is a problem of long standing and we will not attempt to address it here. Rather, we will simply adopt *ad hoc* the form

$$F_j(W,\vec{p}\,',\vec{p}) = \left[\frac{\Lambda_j^2-m_j^2}{\Lambda_j^2+(\vec{p}\,'-\vec{p})^2}\right]^{n_j}\left(\frac{\Lambda_N^4}{\Lambda_N^4+(W^2/4-E_p^2)^2}\right)^2 \times\left(\frac{\Lambda_N^4}{\Lambda_N^4+(W^2/4-E_{p'}^2)^2}\right)^2; \tag{5}$$

that is, we take the form of Eq. (4) and multiply it by a factor $\Lambda_N^4/[\Lambda_N^4+(W^2/4-E_q^2)^2]$ for each nucleon line with momentum $\vec{q}$ entering or leaving the interaction. In all cases except as noted in Table II below we take $n_j=2$.

This form provides the potential with both *t*- and *s*-channel cutoffs. Although it does not remove the objection, raised above, of mixing contact terms into higher partial waves, we shall mitigate that effect via the proviso that the parameter Λ_j for meson terms whose interactions include contact terms be chosen large enough so as to have negligible effects in partial waves with orbital angular momentum $l\geqslant 2$, except for $^3D_1$ because of its coupling to $^3S_1$.

As there are free and nearly free parameters in the models, a simple comparison of the NN phase shifts produced by the four models for a given set of parameters would not, in our opinion, be a useful way to present the results of our investigation. Such a comparison might be seen to favor one model over another, which is not our intention.

Instead, for each of the four models, we perform a constrained least-squares fit of the adjustable parameters to the NN phase shifts in the range of laboratory kinetic energies

TABLE II. Parameters for the TOPT models. The columns labeled PV and PS represent, respectively, the values for the model with pseudovector and pseudoscalar coupling of the π and η mesons, as in the figures. Fixed parameters are shown in parentheses. The values of searched parameters are determined by a least-squares fit to the SP40 *NN* phase shift analysis of Ref. [35]. For these models $n_\pi = 1$ [see Eq. (5)].

Coupling constant	PV	PS	Cutoff	PV (GeV)	PS (GeV)
$g_\pi^2/4\pi$	(13.8)	(13.8)	Λ_π	2.50	1.80
$g_\eta^2/4\pi$	2.15	2.00	Λ_η	1.00	1.21
$g_\sigma^2/4\pi$	6.4355	7.1572	Λ_σ	10.00	9.80
$g_{a_0}^2/4\pi$	0.8463	1.7915	Λ_{a_0}	2.50	1.50
$g_\rho^2/4\pi$	1.14	1.06	Λ_ρ	1.45	1.73
f_ρ/g_ρ	5.12	4.40			
$g_\omega^2/4\pi$	17.40	22.20	Λ_ω	1.41	1.35
f_ω/g_ω	(0)	(0)			
			Λ_N [a]	(0.7)	(0.7)

[a]See Sec. II, Eq. (5) for the use of Λ_N.

TABLE III. Parameters for the Thompson equation models. The columns labeled TPV and TPS represent, respectively, the values for the model with pseudovector and pseudoscalar coupling of the π and η mesons, as in the figures. Fixed parameters are shown in parentheses. The values of searched parameters are determined by a least-squares fit to the SP40 *NN* phase shift analysis of Ref. [35].

Coupling constant	TPV	TPS	Cutoff	TPV (GeV)	TPS (GeV)
$g_\pi^2/4\pi$	(13.8)	(13.8)	Λ_π	2.00	1.80
$g_\eta^2/4\pi$	4.22	5.00	Λ_η	1.00	1.00
$g_\sigma^2/4\pi$	6.8822	7.2057	Λ_σ	10.00	10.00
$g_{a_0}^2/4\pi$	5.1165	5.0071	Λ_{a_0}	2.50	1.50
$g_\rho^2/4\pi$	0.800	0.800	Λ_ρ	1.34	1.31
f_ρ/g_ρ	6.89	6.89			
$g_\omega^2/4\pi$	25.00	25.00	Λ_ω	1.245	1.260
f_ω/g_ω	(0)	(0)			
			Λ_N	(0.7)	(0.7)

from 20 to 300 MeV taken from the energy independent *NN* phase shift analysis SP40 of Ref. [35]. By ''constrained'' we mean that the parameters that are allowed to vary, such as coupling constants and cutoff masses, are restricted to a range that is consistent with values used in the various meson-exchange models of the *NN* interaction in the literature. The results of these best fits will then be compared in detail. We will also, for the sake of completeness, make a comparison of pseudovector and pseudoscalar coupling in the TOPT models with identical parameter sets.

Admittedly, this is not a rigorous procedure, but it reflects better the intention of our work. We wish to examine whether the terms that, in principle, should be included in one-boson exchange models based on TOPT but have heretofore been omitted require a major reworking of previous models, or if their effects can be compensated for by relatively small adjustments in the parameters of the other models. Therefore we are not concerned with ''high precision'' fits of the models to the phase shifts, but with qualitatively acceptable fits of the magnitudes and energy dependencies of the model results to the data, since further refinements of the models, such as the inclusion of two-pion exchange or effects of baryon resonances [33], would necessitate refitting of the parameters and, presumably, result in quantitatively better fits.

At this point we must inject a word of caution for the reader. As our models have both *s*- and *t*-channel cutoffs to regulate the integral equations, one should not expect the cutoff masses that we use, especially those for the mesonic form factors, to agree well with those in the literature for models using different cutoff schemes. The way that cutoffs are implemented in any model is part of the model and thus has a large influence on the values of the model's parameters.

Our procedure is first to select the parameters in the models that we wish to vary and then set the limits of variation of each of these parameter to values that we consider reasonable. For example the πN coupling constant, $g_\pi^2/4\pi$ is fixed at 13.8, whereas the ηN coupling constant, $g_\eta^2/4\pi$, since it is less well known, is allowed to vary from 0 to 6. Cutoff masses Λ_j are allowed a fairly large range, but are required to be greater than 1 GeV. The meson masses are fixed at the values given in Table I. For the nucleonic cutoff mass, Λ_N, we explored a range of values and found that good fits with all the models could be obtained for Λ_N between 600 and 900 MeV. For values below 600 MeV the potential was too strongly suppressed and for values above 1 GeV the cutoff had almost no effect. We therefore fixed the value of Λ_N at 700 MeV in all the models. With this choice the contributions to the scattering amplitude at low c.m. energies from intermediate states with energies above the pion production threshold are strongly suppressed. (We should remark here that this value of Λ_N is of the same order of magnitude as the *s*-channel cutoff employed by Epelbaum *et al.* [15] in their effective field-theoretic approach.) We then perform a least squares search on the variable parameters.

III. RESULTS

The parameters for our four models are shown in Table II, where we give the complete set of coupling constants and cutoff masses for the TOPT models, and in Table III, where we show them for the models based on the Thompson equation [31]. The phase shifts predicted by the various models we have considered are shown in Fig. 3, where we present the results for the TOPT models, and in Fig. 4, where we present them for the Thompson equation models and, for purposes of comparison, also for the TOPT model with pseudovector coupling. Phase shifts are shown for partial waves only up to $J=3$, omitting ϵ_3, since the differences between the phase shifts calculated with the various models are almost imperceptible in the omitted phase shifts. Since the pion coupling is the same in all models, it is clear that the higher partial waves in the energy regime considered are practically identical. The deuteron properties calculated from the models are given in Table IV.

As our primary interest is in the differences due to alter-

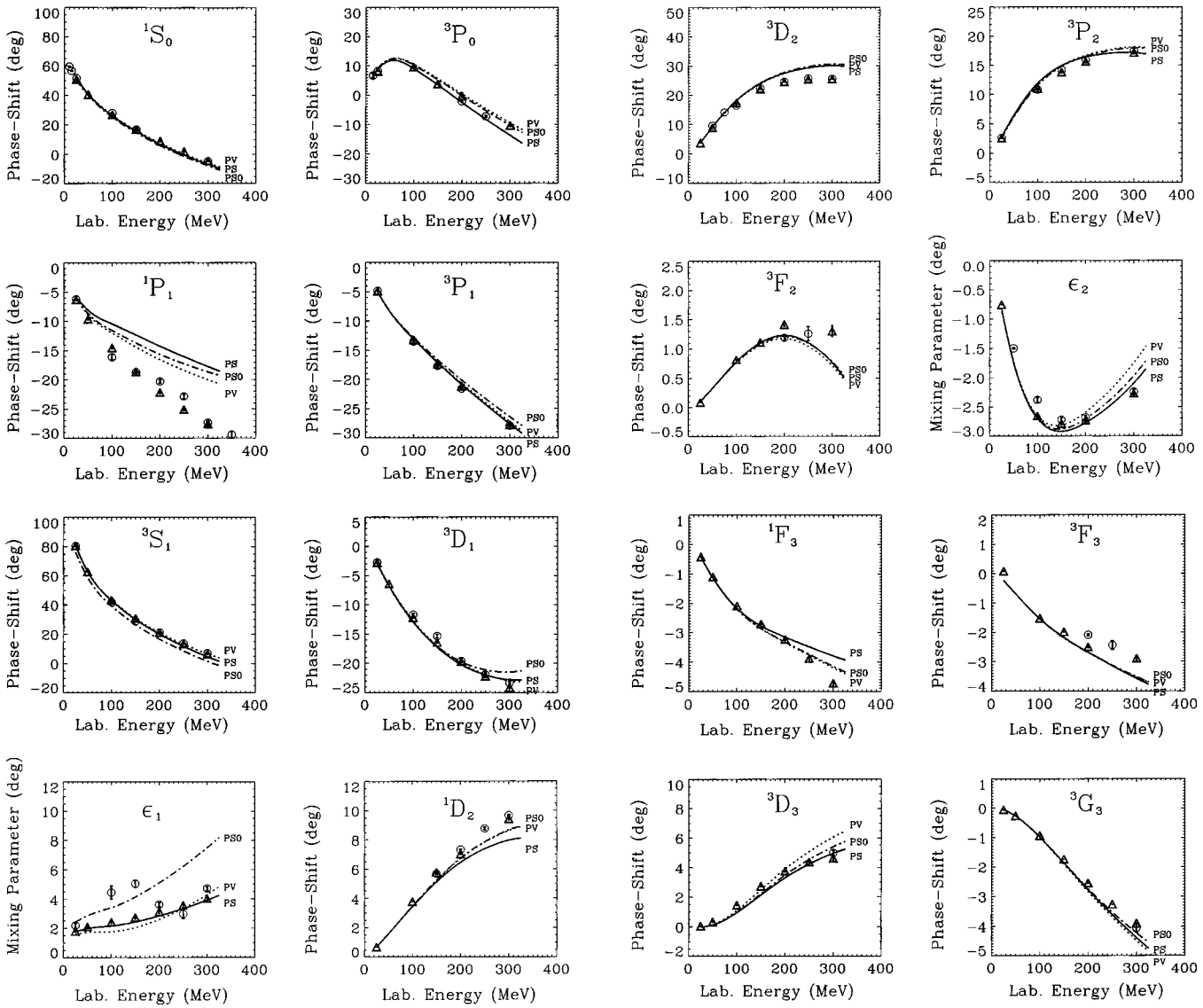

FIG. 3. Phase shifts for TOPT models. The curves labeled PV are the results of the best fit for the model with pseudovector coupling of the π and the η; those labeled PS are the best fit for pseudoscalar coupling. The curves labeled PS0 are the results of using the parameter set of PV but with pseudoscalar coupling. Parameters for the models are given in Table II. The triangles represent the phase shift analysis by the Nijmegen Group at selected energies [36], and the open circles stand for the energy independent analysis SP40 from the CNS DAC Services SAID [35].

native couplings of the pseudoscalar mesons, we shall first examine the results for the TOPT models. We shall then turn our attention to the results of Thompson equation models. Afterwards, we shall briefly compare the results of the models in the two approaches.

A. TOPT models

The two ''best fit'' TOPT models—curves PV and PS in Fig. 3—both give reasonably good descriptions of the phase shift data. Where there are discernible differences, it is difficult to form a consistent picture of the effects of the two alternative couplings that cannot be compensated by relatively small adjustments in the cutoffs or in the coupling constants of the other mesons. As mentioned before, the pion coupling constant is the same in all models. In order to demonstrate the difference of the two coupling schemes as it arises when there is no readjustment of the other meson parameters, Fig. 3 includes the results of a calculation, labeled PS0, in which the only difference from model PV is the change of the coupling of the π and η mesons from pseudovector to pseudoscalar. A comparison of the results of PV with PS0 shows that, even with no readjustments of the cutoffs or coupling constants of the other mesons, the differences between pseudovector and pseudoscalar coupling for π and η is quite small, especially at low energy.

There is, however, one glaring exception to this generalization: the predictions for coupled channels $^3S_1$–$^3D_1$ and the mixing parameter ϵ_1. This parameter, as calculated from PS0 is, almost double the value from PV—and the data—throughout the energy range shown, thus indicating that the tensor forces resulting from the two coupling schemes are

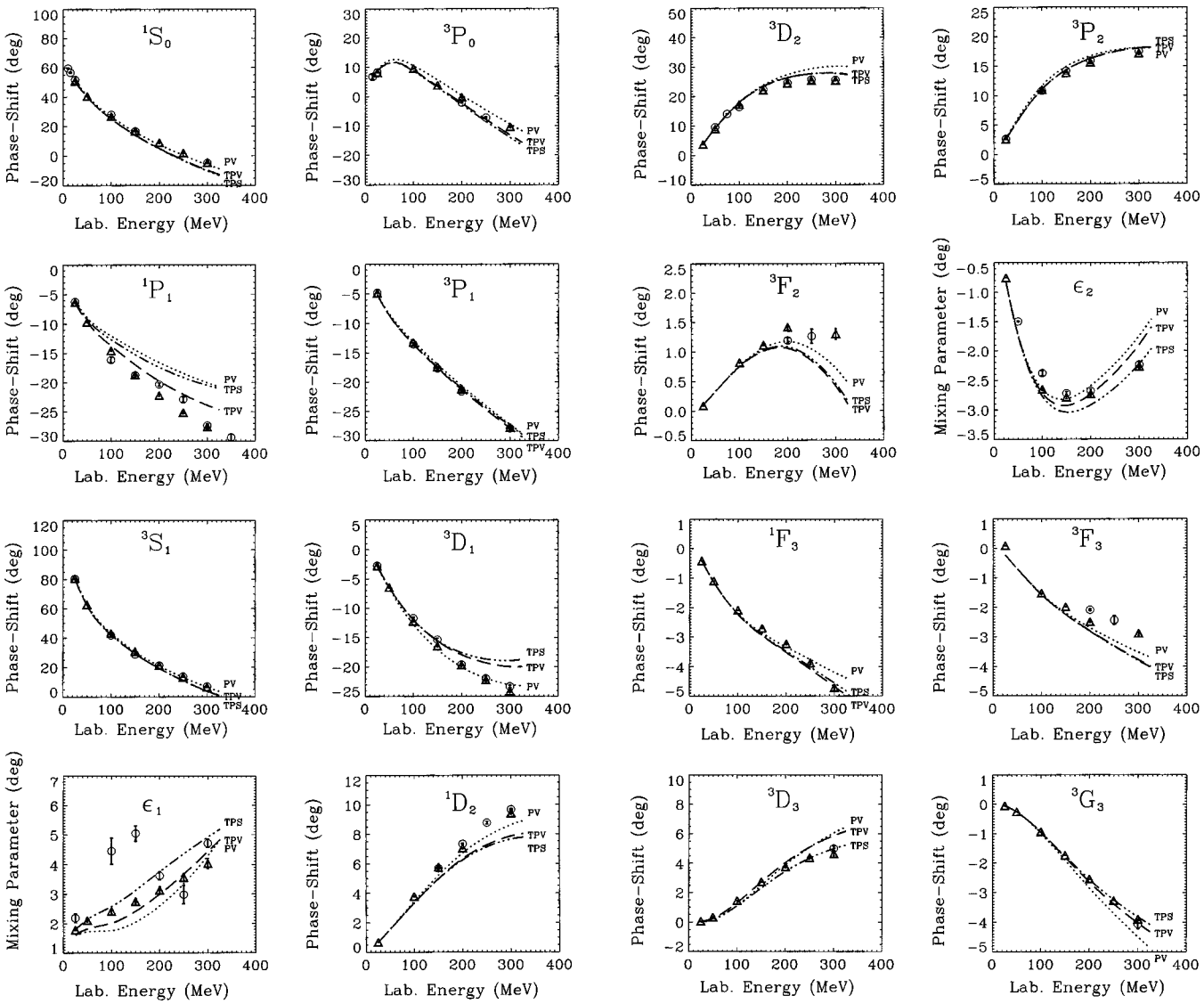

FIG. 4. Phase shifts for Thompson equation models. The curves labeled TPV are the results of the best fit for the model with pseudovector coupling of the π and the η; those labeled TPS are the best fit for pseudoscalar coupling. Included for purposes of comparison are the results of the best fit of the TOPT model with pseudovector coupling (curves labeled PV). Parameters for the models are given in Table II. The error bars are the same as in Fig. 3.

rather different. Confirmation of this conclusion is provided by an examination of the singlet and triplet phase shifts: In the $^1S_0$ and $^1D_2$ the results of models PV and PS0 are almost identical, whereas in $^3S_1$, and in $^3D_1$ at higher energy, there are small—but noticeable—differences between the results for the two models. As the only difference between the two models is in the change from pseudovector to pseudoscalar coupling of the π and η, the effect must be due primarily to a change in the tensor—as opposed to the spin-spin—component of the one-pion exchange interaction.

Indeed, it is the need to describe ϵ_1 more accurately that largely drives the changes in the coupling constants and cut-

TABLE IV. Deuteron properties calculated with the four models considered.

Quantity	Experiment	PV	PS	TPV	TPS
$-E_d$ [MeV]	2.245 75(9) [37]	2.224 47	2.224 46	2.224 66	2.224 54
P_D [%]		3.8	3.4	4.4	3.9
Q_d[fm^2][a]	0.2859(3) [38,39]	0.2784	0.2779	0.2765	0.2754
A_S [fm$^{-1/2}$]	0.8846(9) [38,40]	0.9117	0.9119	0.8974	0.8950
A_D/A_S	0.0256(4) [41]	0.0255	0.0260	0.0252	0.0257

[a]Theoretical values do not include meson exchange current contributions.

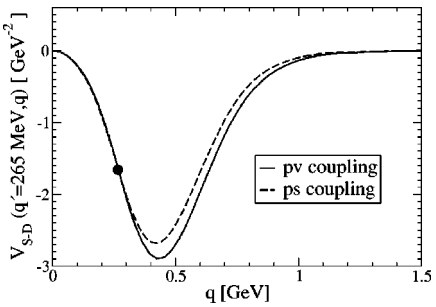

FIG. 5. The $^3S_1-^3D_1$ transition potential, V_{S-D} for the TOPT models PV (pv coupling) and PS0 (ps coupling), with $q'=265$ MeV. The dot in the figure indicates the on-shell point, $q=q'$.

offs in model PS from model PV. With very few exceptions, the results of PS0 are closer than those of PS to the results of PV. The exceptions, as one might expect from their connection with ϵ_1, are the phase shifts $^3S_1$ and $^3D_1$, to which ϵ_1 is coupled.

The main features of the difference between models PV and PS0 can be seen in Fig. 5, where we show the potential for the $^3S_1-^3D_1$ transition for each model as implemented in our approach, for a c.m. momentum of 265 MeV. For near on-shell values of the half-shell momentum the two potentials are nearly the same. As the half-shell momentum gets further from the on-shell point, the difference between PV and PS0 grows larger until, at sufficiently high momenta, the form factors assert their effect, suppressing the differences as both potentials approach zero.

Comparing the coupling constants and cutoffs of PV and PS, one sees that the η is essentially unchanged. The ρ coupling in PS is slightly smaller, but that is partially offset by a cutoff mass that is slightly larger. The greatest differences between the parameters in the two models are in the σ and ω. The ω coupling in PS is about 25% larger than in PV, although its cutoff mass is smaller, which tends to compensate for the increased repulsive strength at short distance. The increase in the σ coupling is necessary, apparently, to provide attraction at intermediate range to counter the greater repulsion due to the ω.

While the picture is not entirely clear, the competition between increased attraction due to the larger σ contribution at intermediate range and increased repulsion at short range due to the larger ω contribution appears evident. In the mid-peripheral uncoupled phases where differences can be observed, i.e., $^1D_2$ and $^3D_2$, PS is slightly more repulsive than PV, while in the more peripheral phase shift $^1F_3$, the reverse is true. For higher partial waves, which are not shown in the figures, the phases are almost entirely given by the on-shell pion exchange term, but the effect is, as one would expect, the same as in $^1F_3$, although the differences are so small as to be invisible on graphs.

B. Thompson equation models

The phase shift fits for the two models that employ the Thompson equation are shown in Fig. 4, along with the results for the TOPT-based model PV discussed in the previous section. The curves labeled TPV show the results for the model with pseudovector coupling of the π and η mesons, while those labeled TPS show the results for the model with pseudoscalar coupling of the π and η mesons. Both TPV and TPS are best-fit results in the restricted sense discussed in Sec. II, in which bounds are placed on the range of the adjustable parameters.

As in the case of the TOPT models, the phase parameter that shows the most striking difference between pseudovector and pseudoscalar coupling is the mixing parameter ϵ_1. Using the models with the Thompson equation with the cutoffs implemented as we have described, it is impossible to achieve a satisfactory description of ϵ_1 while simultaneously keeping the coupling constants within reasonable bounds when pseudoscalar coupling is used for the π and η mesons.

Apart from ϵ_1, the only other phase shifts that reveal any noticeable difference between pseudovector and pseudoscalar coupling in the Thompson equations models are $^1P_1$, ϵ_2, and $^3D_3$, and even there the differences are rather small. For the most part, the two Thompson equation results are closer to each other than either is to PV or to PS. This result is not surprising, since most of the parameters in TPV and TPS are the same, which reflects the fact that they are at the limits of their permitted ranges. An interesting result is that the *t*-channel cutoff of the σ meson Λ_σ is extremely large—10 GeV, which is effectively infinite. This suggests that the *s*-channel cutoff has a very powerful effect in the Thompson equation models, and the large value of Λ_σ reflects an effort of the fitting program to increase the attractive effect of the σ exchange contribution to counter the increased strength of the ω contribution. Indeed, with very few exceptions, both of the Thompson models are more repulsive than PV, as one might expect from the large value of g_ω^2.

A slightly different view of the models that we have considered is provided by the deuteron parameters compiled in Table IV, which shows some small—but consistent— differences between them. All four models are adjusted to fit the deuteron binding energy very accurately. Both TOPT models give a very good value of the quadrupole moment with a relatively low *d*-state probability, which is characteristic of TOPT models, although the tendency of the Thompson models to have relatively large *d*-state probability is mitigated here, presumably because of the strong *s*-channel cutoff that was not present in earlier work [25]. In both the TOPT and Thompson equation models, pseudoscalar coupling results in a lower *d*-state probability than pseudovector coupling. The value of P_D is consistently 0.4–0.5% higher with pseudovector coupling than with pseudoscalar coupling *within the same approach*, as long as the deuteron binding energy is fit to its experimental value and the coupling constants are within their allowed ranges. For example, model PS0, after g_σ^2 is readjusted to give the correct deuteron binding energy, yields almost exactly the same P_D as model PS. The asymptotic *s* wave, A_S, is somewhat high for the TOPT models, although the asymptotic *d*-to-*s* ratio, A_D/A_S, is acceptable. As expected, the *d*-state probability of the Thompson models is larger than in the corresponding TOPT models, resulting in a lower value of A_S. The value of A_D/A_S, however, is not very different among the four models, which

probably explains the smaller quadrupole moments for the Thompson equation models: the slightly greater *d*-state probability in the Thompson equation deuteron wave functions is not sufficient to counter the slightly more compact structure of the deuteron that the Thompson equation produces.

IV. SUMMARY AND CONCLUSIONS

It is clearly impossible to draw any general conclusions concerning the effects of pseudoscalar as opposed to pseudovector coupling of pseudoscalar mesons in the *NN* system. Any statements that we make are necessarily qualified by their model dependence. It is nevertheless useful to summarize our approach and findings and to note, if possible, any tendencies within the limited context of the models that we have investigated.

In the first place, we wished to treat pseudovector coupling properly in the TOPT approach, using the Lippmann-Schwinger equation to generate unitary scattering amplitudes from the one-meson exchange amplitudes, and to compare it with pseudoscalar coupling. The presence of contact terms in the pseudoscalar meson exchange terms, as well as in the vector meson exchange terms with tensor coupling, led us to introduce nucleonic—i.e., *s*-channel—form factors in addition to the *t*-channel form factors that are usually employed in meson exchange models of the *NN* interaction.

For the purpose of comparison with a different approach, we examined the difference between the two coupling schemes in the context of a model based on a particular version of three-dimensional reduction of the Bethe-Salpeter equation, the Thompson equation. In this approach the energy denominators and the off-shell continuations of the meson exchange amplitudes differ from those of TOPT. In particular, no contact terms appear. In order to keep the comparison as close as possible, we chose similar form factors to those in the TOPT-based models that we studied.

Within each model we made a restricted best fit to the *NN* data, allowing meson coupling constants and form factors to vary within broad limits chosen with regard to values of these parameters found in earlier works. We also examined the effect of simply changing the pseudovector coupling of the π and η to pseudoscalar, within the TOPT approach.

Not surprisingly, perhaps, most of the differences in the scattering and bound state properties calculated with the various models were quite small, which probably reflects the fact that the cutoffs were strong enough to strongly suppress differences in the off-shell behavior of the two coupling schemes. The most dramatic difference in the TOPT models appeared in the mixing parameter ϵ_1 when the simple change of pseudovector to pseudoscalar coupling was made. This should not be surprising, since the effect of the contact terms is limited to *s* and *p* waves and states coupled to them. The diagonal pion exchange amplitude is rather weak so that it is in the relatively small mixing parameter ϵ_1, which is dominated by π and ρ exchange, that changes in the short-range behavior of the tensor force is most strongly felt. Indeed, most of the differences between the ''best fit'' pseudovector and pseudoscalar models was due to the readjustment of parameters in the latter needed to produce a better fit to ϵ_1.

The same effect was observed in the Thompson equation models, with the largest relative difference between the pseudovector and pseudoscalar coupling versions remaining after refitting coupling constants appearing in ϵ_1. Other differences between the two Thompson equation models were very small, owing in large part to the fact that several of the adjustable parameters were at the limits of their permitted ranges in both cases.

Differences in the deuteron parameters among the models were similarly quite small, with only the slight tendencies in *d*-state probability, quadrupole moment and asymptotic *s*-state predictions noted previously.

The motivation of this study was to see whether, with a very restricted set of models, one type of coupling of the pseudoscalar mesons would be able better to reproduce *NN* scattering data than the other. Within the TOPT approach one might claim that, on the whole, pseudovector coupling yields a slightly better description of the data than pseudoscalar, but not in every partial wave. Within the Thompson models, the differences between pseudovector and pseudoscalar coupling are still smaller. Between the TOPT and Thompson model predictions there is no clear best. We must conclude therefore that the results obtained for *NN* scattering with the models considered in this work present no compelling evidence that one form of coupling of the pseudoscalar mesons to nucleons is favored over the other.

ACKNOWLEDGMENTS

This work was performed in part under the auspices of the U.S. Department of Energy under Contract No. DE-FG02-93ER40756 with the Ohio University.

APPENDIX A: INTERACTION LAGRANGIANS AND HAMILTONIANS

We present here, for the purpose of completeness, the interaction Lagrangian densities and the corresponding interaction Hamiltonian densities for the various meson-nucleon interactions used in this work.

1. Scalar meson

$$\mathcal{L}_{I,s} = -g_s \bar{\psi}\psi\phi_s , \tag{A1}$$

$$\mathcal{H}_{I,s} = -\mathcal{L}_{I,s} . \tag{A2}$$

2. Pseudoscalar meson, pseudoscalar coupling

$$\mathcal{L}_{I,pps} = -ig_p \bar{\psi}\gamma^5\psi\phi_p , \tag{A3}$$

$$\mathcal{H}_{I,pps} = -\mathcal{L}_{I,pps} . \tag{A4}$$

3. Pseudoscalar meson, pseudovector coupling

$$\mathcal{L}_{I,ppv} = -\frac{g_p}{2m_N}\bar{\psi}\gamma^5\gamma^\mu\psi\partial_\mu\phi_p , \tag{A5}$$

$$\mathcal{H}_{I,ppv} = -\mathcal{L}_{I,ppv} + \frac{1}{2}\frac{g_p^2}{4m_N^2}(\bar{\psi}\gamma^5\gamma^0\psi)^2 . \tag{A6}$$

4. Vector meson

Here we take for the free meson Lagrangian the form

$$\mathcal{L}_{0,v}=-\frac{1}{4}F_{\mu\nu}F^{\mu\nu}+\frac{1}{2}m_v^2A_\mu A^\mu, \tag{A7}$$

where $F_{\mu\nu}\equiv\partial_\mu A_\nu-\partial_\nu A_\mu$. We then have

$$\mathcal{L}_{I,v}=-g_v\bar{\psi}\gamma^\mu\psi A_\mu-\frac{f_v}{4m_N}\bar{\psi}\sigma^{\mu\nu}\psi F_{\mu\nu}, \tag{A8}$$

$$\mathcal{H}_{I,v}=-\mathcal{L}_{I,v}+\frac{g_v^2}{2m_v^2}(\bar{\psi}\gamma^0\psi)^2+\frac{1}{2}\frac{f_v^2}{4m_N^2}(\bar{\psi}\sigma^{i0}\psi)^2, \tag{A9}$$

where $\sigma^{\mu\nu}\equiv(i/2)[\gamma^\mu,\gamma^\nu]_-$. We use the Bjorken-Drell conventions, summing on repeated indices and using the Latin letter i to denote spatial indices $1\cdots3$. Isotopic spin notation has been suppressed.

While it is simple to work out the relation between the Hamiltonian density and the Lagrangian density for nonderivative couplings, i.e., for scalar mesons with scalar coupling and pseudoscalar mesons with pseudoscalar coupling, the procedure for other couplings requires some care. For example, in the case of pseudoscalar mesons with pseudovector coupling, the canonical momentum density $\pi(x)$ is given by

$$\pi(x)=\frac{\partial\mathcal{L}}{\partial(\partial\phi/\partial t)}=\frac{\partial\phi}{\partial t}-j_5^0, \tag{A10}$$

where

$$j_5^\mu=\frac{g_p}{2m_N}\bar{\psi}\gamma^5\gamma^\mu\psi, \tag{A11}$$

which arises from $\mathcal{L}_I$. The relation between $\mathcal{H}$ and $\mathcal{L}$,

$$\mathcal{H}=\left(\frac{\partial\phi}{\partial t}\right)\pi(x)-\mathcal{L}, \tag{A12}$$

yields

$$\begin{aligned}\mathcal{H}&=\frac{1}{2}\pi(x)^2+\frac{1}{2}[\vec{\nabla}\phi(x)^2]+\frac{1}{2}m_\pi^2\phi(x)^2-\vec{j}_5(x)\cdot\vec{\nabla}\phi(x)\\&\quad+j_5^0\pi(x)+\frac{1}{2}[j_5^0(x)]^2+\text{nucleon kinetic terms}\\&=\mathcal{H}_0+\mathcal{H}_I,\end{aligned} \tag{A13}$$

with

$$\mathcal{H}_I=j_5^0(x)\pi(x)-\vec{j}_5(x)\cdot\vec{\nabla}\phi(x)+\frac{1}{2}[j_5^0(x)]^2. \tag{A14}$$

To complete the transformation, one identifies $\pi(x)$ with $\partial_0\phi=\partial\phi/\partial t$ in the *interaction picture*.

Proceeding in a similar manner for the *vector* mesons, one encounters the complication of having four canonical momentum densities, $\pi^\mu(x)$ with $\pi^0(x)=0$. One must then use the Euler-Lagrange equations to obtain a constraint on A^0 in order to reduce the number of degrees of freedom in A^μ from 4 to 3. Identification of A^0 in the interaction picture with $-(1/2m_v^2)\vec{\nabla}\cdot\vec{\pi}$ completes the transformation and gives the result above. For a detailed derivation of the interaction Hamiltonian densities from Lagrangian densities see, e.g., pp. 318–323 of Ref. [34].

APPENDIX B: MATRIX ELEMENTS OF THE POTENTIAL

We show here the potential matrix elements in time-ordered perturbation theory to second order in the meson-nucleon coupling constants derived from the Hamiltonians in Appendix A. The field-theoretic matrix element for the contribution of meson j is multiplied by a cutoff function $F_j(W,\vec{p}\,',\vec{p})$, as described in Sec. II.

We use the helicity basis in the two-nucleon center-of-mass (c.m.) frame. The total c.m energy of the system is W, the momenta of the ingoing and outgoing nucleons are $(\vec{p},-\vec{p})$ and $(\vec{p}\,',-\vec{p}\,')$ with corresponding energies E_p and $E_{p'}$ and helicities λ_1, λ_2 and λ_1', λ_2', with $\lambda=\pm\frac{1}{2}$. The energy transfer in the interaction is $\delta=E_{p'}-E_p$, the three-momentum transfer in the interaction is $\vec{k}=\vec{p}-\vec{p}\,'$ and the energy of the exchanged meson of type j is $\omega_k^j=\sqrt{\vec{k}^2+m_j^2}$. The energy denominator for the meson exchange term is given by $D^j\equiv W-E_p-E_{p'}-\omega_k^j$.

1. Scalar meson

$$V_s^{(2)}=\frac{g_s^2}{(2\pi)^3}I_{12}\frac{1}{\omega_k^sD^s}\{[\mathbf{1}]_1[\mathbf{1}]_2\}F_s(W,\vec{p}\,',\vec{p}). \tag{B1}$$

2. Pseudoscalar meson, pseudoscalar coupling

$$V_{p(ps)}^{(2)}=-\frac{g_p^2}{(2\pi)^3}I_{12}\frac{1}{\omega_k^pD^s}\{[\gamma^5]_1[\gamma^5]_2\}F_{p(ps)}(W,\vec{p}\,',\vec{p}). \tag{B2}$$

3. Pseudoscalar meson, pseudovector coupling

$$\begin{aligned}V_{p(pv)}^{(2)}=\frac{g_p^2}{(2\pi)^3}I_{12}\Bigg\{&\frac{1}{\omega_k^pD^p}\Bigg(-[\gamma^5]_1[\gamma^5]_2\\&-\frac{\delta}{2m_N}([\gamma^5\gamma^0]_1[\gamma^5]_2+[\gamma^5]_1[\gamma^5\gamma^0]_2)\\&+\frac{(\omega_k^p)^2-\delta^2}{4m_N^2}[\gamma^5\gamma^0]_1[\gamma^5\gamma^0]_2\Bigg)\\&+\frac{1}{4m_N^2}[\gamma^5\gamma^0]_1[\gamma^5\gamma^0]_2\Bigg\}F_{p(pv)}(W,\vec{p}\,',\vec{p}).\end{aligned} \tag{B3}$$

4. Vector meson

$$V_v^{(2)}=\frac{g_v^2}{(2\pi)^3}I_{12}\left\{\frac{1}{\omega_k^v D^v}\left(-g_{\mu\nu}[\gamma^\mu]_1[\gamma^\nu]_2+\frac{(\omega_k^v)^2-\delta^2}{m_v^2}[\gamma^0]_1[\gamma^0]_2\right)+\frac{1}{m_v^2}[\gamma^0]_1[\gamma^0]_2\right\}F_v(W,\vec{p}\,',\vec{p})+\frac{f_v^2}{(2\pi)^3 4m_N^2}I_{12}$$

$$\times\left\{\frac{1}{\omega_k^v D^v}(g_{\mu\nu}[\sigma^{\alpha\mu}(p_1'-p_1)_\alpha]_1[\sigma^{\beta\nu}(p_2'-p_2)_\beta]_2+\delta\{[\sigma^{0i}]_1[\sigma^{\beta i}(p_2'-p_2)_\beta]_2+[\sigma^{\alpha i}(p_1'-p_1)_\alpha]_2[\sigma^{0i}]_2\}\right.$$

$$\left.+[(\omega_k^v)^2-\delta^2][\sigma^{0i}]_1[\sigma^{0i}]_2)+[\sigma^{0i}]_1[\sigma^{0i}]_2\right\}F_v(W,\vec{p}\,',\vec{p})+\frac{g_v f_v}{(2\pi)^3 2m_N}I_{12}\frac{1}{\omega_k^v D^v}\{g_{\mu\nu}\{[\gamma^\mu]_1[\sigma^{\alpha\nu}(p_2'-p_2)_\alpha]_2$$

$$+[\sigma^{\alpha\mu}(p_1'-p_1)_\alpha]_1[\gamma^\nu]_2\}+\delta([\gamma^i]_1[\sigma^{0i}]_2+[\sigma^{0i}]_1[\gamma^i]_2)\}F_v(W,\vec{p}\,',\vec{p}). \tag{B4}$$

In the expressions above we have used the compressed notation

$$V_j^{(2)}\equiv\langle\vec{p}\,'\lambda_1'\lambda_2'|V_j^{(2)}(W)|\vec{p}\lambda_1\lambda_2\rangle \tag{B5}$$

and

$$[\mathbf{A}]_1[\mathbf{B}]_2\equiv[\overline{u}(\vec{p}\,',\lambda_1')\mathbf{A}u(\vec{p},\lambda_1)][\overline{u}(-\vec{p}\,',\lambda_2')\mathbf{B}u(-\vec{p},\lambda_2)] \tag{B6}$$

for the matrix elements of the potential.

The isospin factor I_{12} is 1 or $\vec{\tau}_1\cdot\vec{\tau}_2$ as the isospin of the meson concerned is 0 or 1. The normalization of the Dirac spinors is

$$u^\dagger(\vec{p},\lambda)u(\vec{p},\lambda)=1, \tag{B7}$$

and the four-vectors p_1 and p_2 are $(E_p,\vec{p})$ and $(E_p,-\vec{p})$, respectively, and similarly for the primed quantities.

We have written the matrix elements in a way to distinguish clearly the meson exchange terms, which contain energy denominators $D^j=W-E_{p'}-E_p-\omega_k^j$, from the contact terms, which do not. The equivalence of the fully on-shell one-pion exchange with pseudovector coupling with that of the one with pseudoscalar coupling is then evident. In that case $E_p=E_{p'}=W/2$, $D^p=-\omega_k^p$ and $\delta=0$. The term containing $(\omega_k^p)^2$ is exactly canceled by the contact term.

APPENDIX C: THE THOMPSON EQUATION

Matrix elements for the potential to be used in the Thompson equation can easily be found using the results of Appendix B by applying the following prescription:

(i) Change the nucleon spinor normalization to

$$\overline{u}(\vec{p},\lambda)u(\vec{p},\lambda)=1. \tag{C1}$$

(ii) For each meson contribution $V_j^{(2)}$, replace the energy denominator $\omega_k^j D^j$ according to

$$\omega_k^j D^j\rightarrow-(\omega_k^j)^2=-(\vec{p}\,'-\vec{p})^2-m_j^2\,. \tag{C2}$$

(iii) Drop all contact terms.

This prescription is equivalent to using in the one-boson exchange amplitude in the Thompson equation the usual vector meson propagator,

$$D_{\mu\nu}(k)=i\frac{-g_{\mu\nu}+\dfrac{k_\mu k_\nu}{m_v^2}}{k^2-m_v^2}, \tag{C3}$$

where k is the four-momentum transfer carried by the meson. As used in the Thompson equation, k has only spatial components in the c.m. frame of the two nucleons.

[1] C. M. G. Lattes, G. P. S. Occhialini, and C. F. Powell, Nature (London) **160**, 453 (1947); **160**, 486 (1947).
[2] R. E. Marshak and H. A. Bethe, Phys. Rev. **77**, 506 (1947).
[3] H. Yukawa, Proc. Phys. Math. Soc. Jpn. **17**, 48 (1935).
[4] P. Cziffra, M. H. MacGregor, M. J. Moravcsik, and H. P. Stapp, Phys. Rev. **114**, 880 (1959).
[5] K. A. Brueckner and K. M. Watson, Phys. Rev. **92**, 1023 (1953).
[6] M. Taketani, S. Machida, and S. Onuma, Prog. Theor. Phys. **7**, 45 (1952).
[7] T. Matsui and B. D. Serot, Ann. Phys. (N.Y.) **144**, 107 (1982).
[8] W. Bentz, C. Matulla, and H. Baier, Phys. Rev. C **56**, 2280 (1997).
[9] M. Lacombe *et al.*, Phys. Rev. D **12**, 1495 (1975).
[10] A. D. Jackson, D. O. Riska, and B. Verwest, Nucl. Phys. **A249**, 397 (1975).
[11] V. Bernard, N. Kaiser, and U.-G. Meißner, Nucl. Phys. **A615**, 483 (1997).
[12] D. Drechsel and L. Tiator, J. Phys. G **18**, 449 (1992).
[13] S. K. D. Drechsel, O. Hanstein, and L. Tiator, Nucl. Phys.

A645, 145 (1999).
[14] C. Ordóñez, L. Ray, and U. van Kolck, Phys. Rev. Lett. **72**, 1982 (1994).
[15] C. Ordóñez, L. Ray, and U. van Kolck, Phys. Rev. C **53**, 2086 (1996).
[16] E. Epelbaum, W. Glöckle, and U.-G. Meißner, Nucl. Phys. **A637**, 107 (1998).
[17] U.-G. Meißner, E. Epelbaum, and W. Glöckle, Nucl. Phys. **A684**, 371 (2001).
[18] D. R. Entem and R. Machleidt, Phys. Lett. B **524**, 93 (2002).
[19] Rev. Mod. Phys. **39**, 495 (1967).
[20] Suppl. Prog. Theor. Phys. **39** (1967).
[21] Adv. Nucl. Phys. **2**, 223 (1969).
[22] K. Erkelenz, Phys. Rep., Phys. Lett. **13C**, 191 (1974).
[23] K. Kotthoff, K. Holinde, R. Machleidt, and D. Schütte, Nucl. Phys. **A242**, 429 (1975).
[24] K. Holinde and R. Machleidt, Nucl. Phys. **A247**, 495 (1975).
[25] K. Holinde and R. Machleidt, Nucl. Phys. **A256**, 479 (1976).
[26] R. Machleidt, Adv. Nucl. Phys. **19**, 189 (1989).
[27] V. G. J. Stoks, R. A. M. Klomp, C. P. F. Terheggen, and J. J. de Swart, Phys. Rev. C **49**, 2950 (1994).
[28] R. Machleidt, Phys. Rev. C **63**, 024001 (2001).
[29] E. E. Salpeter and H. A. Bethe, Phys. Rev. **84**, 1232 (1951).
[30] R. Blankenbecler and R. Sugar, Phys. Rev. **142**, 1051 (1966).
[31] R. H. Thompson, Phys. Rev. D **1**, 110 (1970).
[32] R. Brockmann and R. Machleidt, Phys. Rev. C **42**, 1965 (1990).
[33] R. Machleidt, K. Holinde, and C. Elster, Phys. Rep. **149**, 1 (1987).
[34] S. Weinberg, *The Quantum Theory of Fields* (Cambridge University Press, Cambridge, England, 1995), Vol. I.
[35] CNS DAC Services (http://gwdac.phys.gwu.edu).
[36] Nijmegen Analysis NN-Online (http://nn-online.sci.kun.nl/nn).
[37] C. van der Leun and C. Alderlisten, Nucl. Phys. **A380**, 261 (1982).
[38] T. Ericson and M. Rosa-Clot, Nucl. Phys. **A405**, 497 (1983).
[39] D. Bishop and L. Cheung, Phys. Rev. A **20**, 381 (1979).
[40] J. J. de Swart, C. P. F. Terheggen, and V. G. J. Stoks, nucl-th/9509032.
[41] N. Rodning and L. Knutson, Phys. Rev. Lett. **57**, 2248 (1986).